AD-A075 201 CAMBRIDGE ACOUSTICAL ASSOCIATES INC MA F/G 20/1
STRUCTURE-BORNE NOISE AND SOUND RADIATION ASSOCIATED WITH A POI--ETC(U)
FEB 79 W T ELLISON , J M GARRELICK N00014-78-C-0218
UNCLASSIFIED CAA-U-600-260 NL

| OF |

AD
A075201

END
DATE
FILMED
11-79
DDC

CAMBRIDGE ACOUSTICAL ASSOCIATES

STRUCTURE-BORNE NOISE AND SOUND RADIATION ASSOCIATED WITH A POINT DRIVEN GRID SUPPORTED INFINITE PLATE

Prepared by:
W. T. Ellison
and
J. M. Garrelick

February 1979

Report U-600-260
Prepared for Office of Naval Research
Structural Mechanics - Code 474
800 North Quincy Street
Arlington, Virginia 22217
Attention: N. Basdekas

54 RINDGE AVENUE EXT., CAMBRIDGE, MASSACHUSETTS 02140

UNCLASSIFIED

SECURITY CLASSIFICATION OF THIS PAGE (When Data Entered)

REPORT DOCUMENTATION PAGE

READ INSTRUCTIONS BEFORE COMPLETING FORM

1. REPORT NUMBER

2. GOVT ACCESSION NO.

3. RECIPIENT'S CATALOG NUMBER

4. TITLE (and Subtitle)

6 STRUCTURE-BORNE NOISE AND SOUND RADIATION ASSOCIATED WITH A POINT DRIVEN GRID SUPPORTED INFINITE PLATE,

5. TYPE OF REPORT & PERIOD COVERED

9 FINAL rept.

6. PERFORMING ORG. REPORT NUMBER

14 CAA — U-600-260

7. AUTHOR(s)

10 W. T. Ellison [redacted] J. M. Garrelick

8. CONTRACT OR GRANT NUMBER(s)

15 N00014-78-C-0218 (new)

9. PERFORMING ORGANIZATION NAME AND ADDRESS

Cambridge Acoustical Associates, Inc.
54 Rindge Avenue Extension
Cambridge, MA 02140

10. PROGRAM ELEMENT, PROJECT, TASK AREA & WORK UNIT NUMBERS

11. CONTROLLING OFFICE NAME AND ADDRESS

Office of Naval Research, Code 474
800 N. Quincy Street
Arlington, VA 22217

12. REPORT DATE

11 Feb~~ruary~~ 1979

13. NUMBER OF PAGES

14. MONITORING AGENCY NAME & ADDRESS(if different from Controlling Office)

12 45

15. SECURITY CLASS. (of this report)

UNCLASSIFIED

15a. DECLASSIFICATION/DOWNGRADING SCHEDULE

16. DISTRIBUTION STATEMENT (of this Report)

Distribution list attached to report supplied by ONR.

DISTRIBUTION STATEMENT A
Approved for public release;
Distribution Unlimited

17. DISTRIBUTION STATEMENT (of the abstract entered in Block 20, if different from Report)

18. SUPPLEMENTARY NOTES

19. KEY WORDS (Continue on reverse side if necessary and identify by block number)

Structural Vibration
Acoustics
Structural Impedance
Radiated Sound
Wave Propagation

20. ABSTRACT (Continue on reverse side if necessary and identify by block number)

A general solution has been developed for the transform responses and the radiated pressure associated with a fluid loaded, orthogonal grid supported plate driven by a harmonic point force. For the case of light or no fluid loading the solution is in a closed form. A particular interest in developing this solution was to determine the structural pass-band characteristics of such a structure in terms of the inertial and elastic properties of the beams composing the grid as well as the plate itself. It is shown that at

next page

DD FORM 1473, 1 JAN 73 · EDITION OF 1 NOV 65 IS OBSOLETE

UNCLASSIFIED

SECURITY CLASSIFICATION OF THIS PAGE (When Data Entered)

072 750

LB

20. Abstract (Continued)

any given frequency there always exist some set of structural wave numbers $(k_x^{\sqcap}, k_y^{\sqcap})$ that represent freely propagating waves. This result is in contrast to previous one-dimensional analyses that result in specific tests of propagating and nonpropagating bands.

The nature of the response of the structure as a function of frequency is provided in terms of the various inertial and elastic properties of the structure, and an analogy is drawn with the one-dimensional result in terms of propagating wave number sets being confronted with an inertial or compliant impedance. The analogy results in the propagating pass bands flipping about the one-dimensional dlamped-clamped resonant frequencies.

Numerical results are presented comparing the on-axis radiated pressure associated with the one-dimensional and two-dimensional grid structures. For the drive point at a beam location the difference in on-axis radiated pressure is due to the larger inertial impedance of the two-dimensional grid structure.

Accession For	
NTIS GRA&I	✓
DDC TAB	
Unannounced	
Justification Letter on file	
By	
Distribution/	
Availability Codes	
Dist	Avail and/or special
A	

STRUCTURE-BORNE NOISE AND SOUND RADIATION ASSOCIATED WITH A POINT DRIVEN GRID SUPPORTED INFINITE PLATE

Prepared by:
W. T. Ellison
and
J. M. Garrelick

February 1979

Report U-600-260
Prepared for
Office of Naval Research
Structural Mechanics - Code 474
800 North Quincy Street
Arlington, Virginia 22217
Attention: N. Basdekas

Cambridge Acoustical Associates, Inc.
54 Rindge Avenue Extension
Cambridge, Massachusetts 02140

TABLE OF CONTENTS

ABSTRACT

A general solution has been developed for the transform response and the radiated pressure associated with a fluid loaded, orthogonal grid supported plate driven by a harmonic point force. For the case of light or no fluid loading the solution is in a closed form. A particular interest in developing this solution was to determine the structural pass-band characteristics of such a structure in terms of the inertial and elastic properties of the beams composing the grid as well as the plate itself. It is shown that at any given frequency there always exist some set of structural wave numbers (k_x, k_y) that represent freely propagating waves. This result is in contrast to previous one-dimensional analyses that result in specific sets of propagating and nonpropagating bands.

The nature of the response of the structure as a function of frequency is provided in terms of the various inertial and elastic properties of the structure, and an analogy is drawn with the one-dimensional result in terms of propagating wave number sets being confronted with an inertial or compliant impedance. The analogy results in the propagating pass bands flipping about the one-dimensional clamped-clamped resonant frequencies.

Numerical results are presented comparing the on-axis radiated pressure associated with the one-dimensional and two-dimensional grid structures. For the drive point at a beam location the difference in on-axis radiated pressure is due to the larger inertial impedance of the two-dimensional grid structure.

I. INTRODUCTION

One of the basic building blocks of hull or cabin-like structures is the plating-stringer combination. Typically, machinery induced vibratory forces are applied to a stringer through a foundation structure. The vibration field then propagates along the hull via the hull plating as well as the stringers.

Cremer and Heckl[1] and Mead,[2] have analyzed the one-dimensional case, i.e., wave propagation in periodically supported, undamped beams. They showed that within discrete frequency bands waves can propagate freely without decay. Outside these "propagation bands," waves decay with distance. The particular problem considered by Mead assumed that the periodic supports offer infinite translational impedances and spring-like rotational constraints. Under the assumption that the excitation is localized to within a single bay, he found that wave motion is produced in the adjacent bays and that these waves are freely propagating within discrete frequency bands. The purpose of this report is to analyze the cut-off frequencies and pass-bands associated with the two-dimensional problem, namely a point driven orthogonal grid structure, and to interpret those results in terms of the propagation of structure-borne noise and the radiation of sound.

II. ANALYSIS

A. General

The structure to be undertaken in this analysis is that of an infinite plate periodically supported by a square orthogonal grid and submerged in a semi-infinite acoustic medium. The problem to be analyzed is the response of this structure to a single harmonic point force applied to the plate at a grid intersection point. Specifically, we will examine "cut-off" phenomena in terms of the various elastic properties of the structure. The subsidiary result for the case of a one dimensional periodic array of beams supporting the plate is also provided.

The geometry utilized in the analysis is depicted in Fig. II-1a and b.

B. Equations of Motion

In the following development we have assumed a harmonic time dependence of the form, $e^{-i\omega t}$. Derivatives with respect to time in the plate and beam equations have thus been taken, and the time dependence factored out.

1. Thin Plate Equations - Assuming that the force is applied at the origin which is also a grid intersection point, then the equation of motion is,

$$[D\nabla^4 - m_p\omega^2]w_p(x,y) = F_o\,\delta(x)\,\delta(y) + \sum_{n=-\infty}^{\infty} Q(x,y)\,\delta(x-nL) + \sum_{m=-\infty}^{\infty} Q(x,y)\,\delta(y-mL) + p(x,y) \qquad \text{(II-1)}$$

where

$D = E_p h_p^3/12(1-\nu_p^2)$

E_p = Plate modulus of elasticity

h_p = Plate thickness

ν_p = Poisson's Ratio

$m_p = \rho_p h_p$

ρ_p = Density of plate

$k_f^4 = m_p \omega^2 / D$

F_o = Applied Force

$Q(x,y)$ = Beam reaction force

$p(x,y)$ = Fluid pressure reaction on plate

Upon applying the double Fourier transform to Eq. II-1, we obtain

$$LD[(k_x^2+k_y^2)^2-k_f^4]\tilde{w}_p(k_x,k_y) = LF_o + \sum_{n=-\infty}^{\infty} \tilde{Q}\left[\left(k_x - \frac{2\pi n}{L}\right), k_y\right] + \sum_{m=-\infty}^{\infty} \tilde{Q}\left[k_x, \left(k_y - \frac{2\pi m}{L}\right)\right] + \tilde{p}(k_x,k_y) \quad \text{(II-2)}$$

where we have utilized the following transform relations,

$$\tilde{f}(k_x,k_y) = \int_{-\infty}^{\infty}\int_{-\infty}^{\infty} f(x,y)e^{-ik_x x} e^{-ik_y y} \, dxdy$$

$$f(x,y) = \frac{1}{4\pi^2}\int_{-\infty}^{\infty}\int_{-\infty}^{\infty} \tilde{f}(k_x,k_y)\, e^{+ik_x x} e^{+ik_y y} \, dk_x kd_y$$

$$\sum_{n=-\infty}^{\infty} \int_{-\infty}^{\infty} f(x)\,\delta(x-nL)e^{-ik_x x} dx = \frac{1}{L} \sum_{n=-\infty}^{\infty} \tilde{f}\left(k_x - \frac{2\pi n}{L}\right)$$

Now for a plate of infinite extent we can also write the transformed surface pressure in terms of the transformed plate displacement.[3]

$$\tilde{p}(k_x,k_y) = \frac{-i\omega^2\rho\tilde{w}(k_x,k_y)}{(k^2-k_x^2-k_y^2)^{1/2}} \quad \text{(II-3)}$$

where

ρ = Density of surrounding fluid

k = Acoustic wave number in fluid (ω/c)

2. <u>Beam (Grid) Equations</u> - We can write two equations for the grid network of orthogonal (Euler-Bernoulli) beams,

$$[E_B I_B \frac{\partial^4}{\partial y^4} - M_B \omega^2] w_p(x,y)\,\delta(x-nL) = -\,Q(x,y)\,\delta(x-nL) \qquad \text{(II-4)}$$

$$[E_B I_B \frac{\partial^4}{\partial x^4} - M_B \omega^2] w_p(x,y)\,\delta(y-mL) = -\,Q(x,y)\,\delta(y-mL) \qquad \text{(II-5)}$$

where

E_B = Beam modulus of elasticity

I_B = Beam moment of inertia

$M_B = \rho_B A_B$, mass per unit length of beam

$k_B^4 = M_B \omega^2 / E_B I_B$

Applying the double Fourier transform to the two beam equations results in,

$$E_B I_B (k_y^4 - k_B^4)\tilde{w}_p\left[\left(k_x - \frac{2\pi n}{L}\right), k_y\right] = -\,\tilde{Q}\left[\left(k_x - \frac{2\pi n}{L}\right), k_y\right] \qquad \text{(II-6)}$$

$$E_B I_B (k_x^4 - k_B^4)\tilde{w}_p\left[k_x, \left(k_y - \frac{2\pi m}{L}\right)\right] = -\,\tilde{Q}\left[k_x, \left(k_y - \frac{2\pi m}{L}\right)\right] \qquad \text{(II-7)}$$

C. <u>The Coupled Solution</u>

In developing the solution to the coupled equations of motion Eqs. II-2, II-6, and II-7) we have defined the following admittance functions,

$$Y_p(k_x,k_y) \equiv \left[LD[(k_x^2+k_y^2)^2-k_f^4] - \frac{i\omega^2\rho L}{(k^2-k_x^2-k_y^2)^{1/2}} \right]^{-1} \tag{II-8}$$

$$Y_B^x \equiv \left[E_B I_B [k_x^4-k_B^4]\right]^{-1} \quad , \quad Y_B^y \equiv \left[E_B I_B [k_y^4-k_B^4]\right]^{-1} \tag{II-9}$$

and adopted the following notation,

$$k_x^n \equiv k_x - \frac{2\pi n}{L}$$

$$k_x^{n,m} \equiv k_x - \frac{2\pi n}{L} - \frac{2\pi m}{L}$$

$$\hat{F}_o \equiv F_o L$$

$$\sum_n \equiv \sum_{n=-\infty}^{\infty}$$

Using these relations we can write the transformed equations of motion as,

$$Y_p^{-1}(k_x,k_y)\tilde{w}_p(k_x,k_y) = \hat{F}_o + \sum_n \tilde{Q}(k_x^n,k_y) + \sum_m \tilde{Q}(k_x,k_y^m) \tag{II-10}$$

$$\tilde{w}_p(k_x^n,k_y) = - Y_B^y \tilde{Q}(k_x^n,k_y) \tag{II-11}$$

$$\tilde{w}_p(k_x,k_y^m) = - Y_B^x \tilde{Q}(k_x,k_y^m) \tag{II-12}$$

Now we wish to solve for the structure displacement response, $\tilde{w}_p$, in terms of the plate and beam admittance functions, Y_p and Y_B, and the driving force, F_o.

Thus, in Eq. II-10 we first set,

$$k_x = k_x^\ell$$

and then summing both sides over all ℓ, we obtain

$$\sum_{\ell} \tilde{w}_p(k_x^{\ell},k_y) = \hat{F}_o \sum_{\ell} Y_p(k_x^{\ell},k_y) + \sum_n \tilde{Q}(k_x^n,k_y) \sum_{\ell} Y_p(k_x^{\ell},k_y)$$

$$+ \sum_{\ell} Y_p(k_x^{\ell},k_y) \sum_n \tilde{Q}(k_x^{\ell},k_y^n) \qquad \text{(II-13)}$$

Similarily using Eq. II-10 again but now setting $k_y = k_y^{\ell}$ and summing over all ℓ, we obtain,

$$\sum_{\ell} w_p(k_x,k_y^{\ell}) = \hat{F}_o \sum_{\ell} Y_p(k_x,k_y^{\ell}) + \sum_{\ell} Y_p(k_x,k_y^{\ell}) \sum_n \tilde{Q}(k_x^n,k_y^{\ell})$$

$$+ \sum_n \tilde{Q}(k_x,k_y^n) \sum_{\ell} Y_p(k_x,k_y^{\ell}) \qquad \text{(II-14)}$$

In both of these manipulations we have utilized the following identity

$$\sum_n A(n) \sum_m C(n+m) = \sum_m C(m) \sum_n A(n)$$

Now summing over Eq. II-11, and II-12 we have

$$\sum_n \tilde{w}_p(k_x^n,k_y) = -Y_B^y \sum_n \tilde{Q}(k_x^n,k_y) \qquad \text{(II-15)}$$

$$\sum_n \tilde{w}_p(k_x,k_y^n) = -Y_B^x \sum_n \tilde{Q}(k_x,k_y^n) \qquad \text{(II-16)}$$

Substituting Eq. II-15 into II-13, and II-16 into II-14 yields the following set of equations,

$$-Y_B^y \sum_n \tilde{Q}(k_x^n,k_y) = \hat{F}_o \sum_{\ell} Y_p(k_x^{\ell},k_y) + \sum_n \tilde{Q}(k_x^n,k_y) \sum_{\ell} Y_p(k_x^{\ell},k_y)$$

$$+ \sum_{\ell} Y_p(k_x^{\ell},k_y) \sum_n \tilde{Q}(k_x^{\ell},k_y^n) \qquad \text{(II-18)}$$

$$-Y_B^x \sum_{\ell} \tilde{Q}(k_x,k_y^{\ell}) = \hat{F}_o \sum_{\ell} Y_p(k_x,k_y^{\ell}) + \sum_{\ell} Y_p(k_x,k_y^{\ell}) \sum_n \tilde{Q}(k_x^n,k_y^{\ell})$$

$$+ \sum_n \tilde{Q}(k_x,k_y^n) \sum_{\ell} Y_p(k_x,k_y^{\ell}) \qquad \text{(II-19)}$$

To solve for the line reaction transform in terms of the known admittance functions we must make use of the symmetry inherent in the problem. Thus, by symmetry we know,

$$\sum_n \tilde{Q}(k_x^n, k_y) = \sum_n \tilde{Q}(k_y^n, k_x) \qquad \text{(II-20)}$$

Multiplying both sides by $Y_p(k_x, k_y)$, replacing k_y with k_y^m and summing over all m results in the following identity,

$$\sum_m Y_p(k_x, k_y^m) \sum_n \tilde{Q}(k_x^n, k_y^m) = \sum_n \tilde{Q}(k_x^n, k_y) \sum_m Y_p(k_x, k_y^m) \qquad \text{(II-21)}$$

In a parallel development we can show that

$$\sum_n Y_p(k_x^n, k_y) \sum_m \tilde{Q}(k_x^n, k_y^m) = \sum_m \tilde{Q}(k_x, k_y^m) \sum_n Y_p(k_x^n, k_y) \qquad \text{(II-22)}$$

Substituting these two results in Eq. II-18, and II-19 respectively, yields the following pair of equations,

$$-\sum_n \tilde{Q}(k_x^n, k_y)\,[Y_B^y + S_x] = \hat{F}_o S_x + S_y \sum_m \tilde{Q}(k_x, k_y^m) \qquad \text{(II-23)}$$

$$-\sum_m \tilde{Q}(k_x, k_y^m)\,[Y_B^x + S_y] = \hat{F}_o S_y + S_x \sum_n \tilde{Q}(k_x^n, k_y) \qquad \text{(II-24)}$$

where

$$S_x \equiv \sum_n Y_p(k_x^n, k_y) \qquad \text{(II-25)}$$

$$S_y \equiv \sum_m Y_p(k_x, k_y^m) \qquad \text{(II-26)}$$

Solving Eqs. II-23 and II-24 simultaneously for the transform grid reaction sums and substituting into Eq. II-10 we reach the final result for the transform of the displacement response.

$$\tilde{w}_p(k_x, k_y) = Y_p(k_x, k_y)\hat{F}_o \left[\frac{1}{1 + \dfrac{Y_B^x S_x + Y_B^y S_y}{Y_B^x Y_B^y}} \right] \qquad \text{(II-27)}$$

D. The Plate Admittance Sums, S_x and S_y

The result provided by Eq. II-27 is limited to numerical computation by the infinite sums of the plate admittance functions. Examining these sums we have from Eq. II-25,

$$S_x = \sum_{n=-\infty}^{\infty} Y_p(k_n^x, k_y) \quad , \quad S_y = \sum_{m=-\infty}^{\infty} Y_p(k_x, k_y^m)$$

where,

$$[Y_p(k_x^n, k_y)]^{-1} = LD\left\{\left[\left(k_x - \frac{2\pi n}{L}\right)^2 + k_y^2\right]^2 - k_f^4\right\} - \left\{\frac{i\omega\rho L}{\left[k^2 - \left(k_x - \frac{2\pi n}{L}\right)^2 - k_y^2\right]^{1/2}}\right\} \qquad \text{(II-28)}$$

We can see that with fluid loading included this sum will be wholly real for values of, $k^2 < k_x^2 + k_y^2$. For values of $k^2 \geq k_x^2 + k_y^2$ the sum will result in both real and imaginary components.

With the fluid loading the sums must be evaluated numerically. There is no problem with convergence but as higher frequencies are considered more terms will be required. In general the number of terms needed is the order of $2k_fL$.

Neglecting the effect of fluid loading, however, the sums are in the form of a quartic in n.

$$S_x = \left(\frac{1}{LD}\right)\left(\frac{L}{2\pi}\right)^4 \sum_{n=-\infty}^{\infty} \frac{1}{p_x(n, f_x, f_y)} \qquad \text{(II-29)}$$

where,

$$p_x(n, f_x, f_y) = [(f_x - n)^2 + f_y^2]^2 - f_p^4 \qquad \text{(II-30a)}$$

$$f_x = \frac{k_x L}{2\pi} \qquad \text{(II-30b)}$$

$$f_y = \frac{k_y L}{2\pi} \qquad \text{(II-30c)}$$

$$f_p = \frac{k_f L}{2\pi} \qquad \text{(II-30d)}$$

Now the quartic in the denominator of the sum has four roots

$$p_x(n, f_x, f_y) = (n-p_1)(n-p_2)(n-p_3)(n-p_4) \qquad \text{(II-31)}$$

where,

$$p_1 = f_x + \left(f_p^2 - f_y^2\right)^{1/2}$$

$$p_2 = f_x - \left(f_p^2 - f_y^2\right)^{1/2}$$

$$p_3 = f_x + i\left(f_p^2 + f_y^2\right)^{1/2}$$

$$p_4 = f_x - i\left(f_p^2 + f_y^2\right)^{1/2}$$

Therefore using the residue theorem result[4]

$$\sum_{n=-\infty}^{\infty} p(n) = -\{\text{sum of the residues of } \pi p(z)\cot\pi z \text{ at the poles of } p(z)\}$$

we can write the result for S_x without fluid loading.

$$S_x = -\left(\frac{1}{LD}\right)\left(\frac{L}{2\pi}\right)^4\left(\frac{\pi}{4f_p^2}\right)\left\{\frac{\cot\pi[f_x+(f_p^2-f_y^2)^{1/2}]-\cot\pi[f_x-(f_p^2-f_y^2)^{1/2}]}{(f_p^2-f_y^2)^{1/2}}\right. \qquad \text{(II-32)}$$

$$\left. + \frac{i\cot\pi[f_x+i(f_p^2+f_y^2)^{1/2}]-i\cot\pi[f_x-i(f_p^2+f_y^2)^{1/2}]}{(f_p^2+f_y^2)^{1/2}}\right\}$$

The result for S_y is directly obtained by simply switching f_x and f_y in Eq. II-32.

E. The Transform Displacement Response

Using Eq. II-29 with the results just produced, we can write out the transform of the displacement response in a closed form with no infinite sums. The most general expression does not appear to be simply amenable to inverse transformation, however, we can obtain the information on passbands from the behavior of the transform itself. To do this it will be simple and more enlightening to examine our general expression in some of the limiting regions of wavenumber space where the algebraic form of the result is not quite so ponderous. These results are undertaken in the balance of this section.

1. Case #1, $k_f >> k_x, k_y$ - In this case the plate admittance sums are independent of k_x and k_y,

$$S_x = S_y = \frac{-k_f}{4m_p\omega^2}\left[\cot\frac{k_fL}{2} + \coth\frac{k_fL}{2}\right] \tag{II-33}$$

$$y_p(k_x,k_y) = -\frac{1}{Lm_p\omega^2} \tag{II-34}$$

Assuming the beam wavenumber, k_B, to be of arbitrary magnitude,* we can write our solution directly,

$$\tilde{w}_p(k_x,k_y) = -\frac{F_o}{m_p\omega^2}\left\{\frac{1}{1-\frac{\gamma_m}{2}\left[\frac{k_fL}{2}\right]\left[\left(\frac{k_x}{k_B}\right)^4+\left(\frac{k_y}{k_B}\right)^4-2\right]\left[\cot\frac{k_fL}{2}+\coth\frac{k_fL}{2}\right]}\right\} \tag{II-35}$$

The factor, γ_m, represents the ratio of the beam mass to the plate mass. Thus,

$$\gamma_m = M_B/m_pL$$

* For typical beam/plate combinations the ratio of k_B/k_f would be expected to be less than unity.

2. Case #2, $k_f >> k_x, k_y$ and $k_B >> k_x, k_y$ - For this case we can write the answer directly from our previous result, or

$$\tilde{w}_p(k_x,k_y) = -\frac{F_o}{m_p\omega^2}\left\{\frac{1}{1+\gamma_m\left(\frac{k_f L}{2}\right)\left(\cot\frac{k_f L}{2}+\coth\frac{k_f L}{2}\right)}\right\} \tag{II-36}$$

Note that Eq. II-36 is also the solution for the very important case of $k_x, k_y = 0$. This solution, related to the on-axis radiated sound pressure, is discussed in greater detail in Section III.

3. Case #3, $k_x, k_y >> k_f, k_B$, and $k_x L, k_y L >> 1$ - In this instance we have used the results,

$$\lim_{x,y\to\infty} \csc^2(x \pm iy) = 0$$

$$\lim_{x,y\to\infty} \cot(x \pm iy) = \mp i$$

to arrive at greatly simplified expressions for the plate admittance functions,

$$S_x = \frac{1}{4D|k_y|^3}$$

$$S_y = \frac{1}{4D|k_x|^3}$$

and our resultant displacement response is,

$$\tilde{w}_p(k_x,k_y) = \frac{F_o}{m_p\omega^2}\left[\frac{k_f^4}{(k_x^2+k_y^2)^2}\right]\left[\frac{1}{1+\frac{\gamma_m}{4}\left(\frac{k_f}{k_B}\right)^4 L(|k_x|+|k_y|)}\right] \tag{II-37}$$

4. Case #4, $k_x = k_y = k_f$ - This particular case, of course, is limited to a single point instead of a region in wavenumber space. There are two solutions with simplified results,

a. $\underline{k_f L >> 1}$

$$\tilde{w}_p(k_x,k_y) = \frac{F_o}{3m_p\omega^2}\left\{\frac{1}{1+\frac{\gamma_m}{2\sqrt{2}}\left(\frac{k_f L}{2}\right)\left[\sqrt{2}\,k_f L\,\csc^2\left(\frac{k_f L}{2}\right)-1\right]\left[\left(\frac{k_f}{k_B}\right)^4-1\right]}\right\} \quad \text{(II-38)}$$

b. $\underline{k_f L << 1}$

$$\tilde{w}_p(k_x,k_y) = \frac{F_o}{3m_p\omega^2}\left\{\frac{1}{1+\frac{5}{6}\gamma_m\left[\left(\frac{k_f}{k_B}\right)^4-1\right]}\right\} \quad \text{(II-39)}$$

F. One Dimensional Beam Array

A subsidiary result of the preceding analysis for the grid supported plate is the solution for the point driven plate supported by a one dimensional periodic array of beams (Fig. II-1b).

As the result follows directly from the grid analysis we will simply outline the steps beginning with the transformed equation of motion,

Plate

$$y_p^{-1}(k_x,k_y)\tilde{w}_p(k_x,k_y) = \hat{F}_o + \sum_n \tilde{Q}(k_x^n,k_y) \quad \text{(II-40)}$$

Beam

$$y_B^{-1}(k_y)\tilde{w}_p(k_x^n,k_y) = -\tilde{Q}(k_n^x,k_y) \quad \text{(II-41)}$$

where y_p^{-1} and y_B^{-1} are given by Eqs. II-8 and II-9. Using the same approach as followed in developing Eqs. II-13 through II-16, we can reach the following result

$$\sum_n \tilde{Q}(k_x^n,k_y) = \frac{-\hat{F}_o S_x}{y_B^y+S_x} \quad \text{(II-42)}$$

and the transform displacement is

$$\tilde{w}_p(k_x,k_y) = y_p(k_x,k_y)\hat{F}_o \left[\frac{1}{1 + \dfrac{S_x}{y_B(k_y)}}\right] \tag{II-43}$$

where S_x is still provided by the result shown in Eq. II-32. As with the grid solution we can develop the following limiting results.

1. Case #1, $k_f >> k_x,k_y$

$$\tilde{w}_p(k_x,k_y) = -\frac{F_o}{m_p w^2}\left\{\frac{1}{1 - \dfrac{\gamma_m}{2}\left[\dfrac{k_f L}{2}\right]\left[\left(\dfrac{k_y}{k_B}\right)^4 - 1\right]\left[\cot\dfrac{k_f L}{2} + \coth\dfrac{k_f L}{2}\right]}\right\} \tag{II-44}$$

2. Case #2, $k_f >> k_x,k_y$ and $k_B >> k_y$

$$\tilde{w}_p(k_x,k_y) = \frac{F_o}{m_p w^2}\left\{\frac{1}{1 + \dfrac{\gamma_m}{2}\left(\dfrac{k_f L}{2}\right)\left(\cot\dfrac{k_f L}{2} + \coth\dfrac{k_f L}{2}\right)}\right\} \tag{II-45}$$

This, of course, is also the result for $k_x = k_y = 0$.

3. Case #3, $k_x,k_y >> k_f,k_B$ and $k_x L,k_y L >> 1$

$$\tilde{w}_p(k_x,k_y) = \frac{F_o}{m_p w^2}\left[\frac{k_f^4}{(k_x^2+k_y^2)^2}\right]\left[\frac{1}{1 + \dfrac{\gamma_m}{4}\left(\dfrac{k_f}{k_B}\right)^4 |k_y|}\right] \tag{II-46}$$

4. Case #4, $k_x = k_y = k_f$

a. $\frac{k_f L}{2} >> 1$

$$\tilde{w}_p(k_x,k_y) = \frac{F_o}{3m_p w^2}\left[\frac{1}{1 + \frac{\gamma_m}{4\sqrt{2}}\left(\frac{k_f L}{2}\right)\left[2\sqrt{2}\left(\frac{k_f L}{2}\right)\csc^2\left(\frac{k_f L}{2}\right) - 1\right]\left[\left(\frac{k_f}{k_B}\right)^4 - 1\right]}\right] \quad \text{(II-47)}$$

b. $\frac{k_f L}{2} << 1$

$$\tilde{w}_p(k_x,k_y) = \frac{F_o}{3m_p w^2}\left[\frac{1}{1 + \frac{5}{12}\ \gamma_m\left[\left(\frac{k_f}{k_B}\right)^4 - 1\right]}\right] \quad \text{(II-48)}$$

FIGURE II-1a GRID-SUPPORTED PLATE GEOMETRY

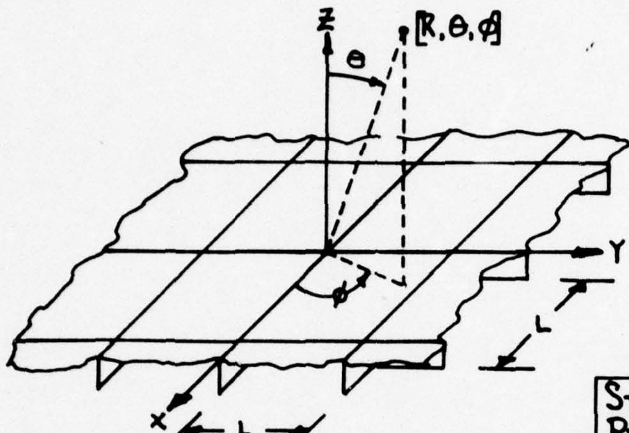

PLATE SUPPORTED BY
PERIODIC GRID OF BEAMS AT:
$X = \pm nL, \quad n = 0, 1, 2, \cdots, \infty$
$Y = \pm mL, \quad m = 0, 1, 2, \cdots, \infty$

STRUCTURAL PROPERTIES	SYMBOL	
	PLATE	BEAMS
THICKNESS	h_P	—
DENSITY	ρ_P	ρ_B
MODULUS	E_P	E_B
DAMPING	η_P	η_B
SECT. AREA	—	A_B
MOM. INERTIA	—	I_B
DRIV. FORCE	$F_0 e^{-i\omega t}$	

FIGURE II-1b ARRAY-SUPPORTED PLATE GEOMETRY

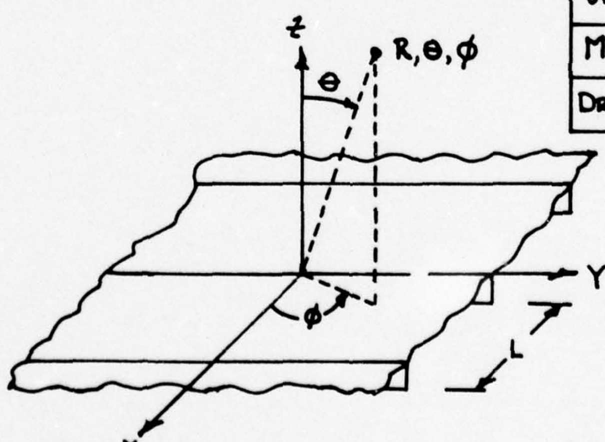

PLATE SUPPORTED BY
PERIODIC ARRAY OF BEAMS AT:
$X = \pm nL, \quad n = 0, 1, 2, \cdots, \infty$

III. PASS BAND CHARACTERISTICS

In the analysis section we developed the transform displacement response for two infinitely periodic structures; a plate supported by a one-dimensional array of beams, and a plate supported by a two-dimensional square grid of beams. In both cases the structure was driven by a point force located at a beam support location, and in the grid case at a grid intersection point as well. One of the purposes of this analysis was to determine if such structures exhibited characteristic "pass-bands" within which energy freely propagated from the drive point throughout the structure. In a complementary sense the determination of the existence of non-propagating bands, within which energy was trapped in the bays adjacent to the drive point, was also desired. The purpose of this section will be to determine if such band characteristics exist for the two classes of structures investigated. This is accomplished by investigating the singularities in the wave number spectrum of the plating response. A given frequency will be considered to be within a pass band if, at that frequency, singularities exist which fall on the real (k_x,k_y) axes thus representing undamped propagating waves. Examining the limiting solution $(k_x,k_y << k_f)$ as represented by Eq. II-35, we have

$$\tilde{w}_p(k_x,k_y) = \frac{F_o}{m_p\omega^2}\left\{\frac{1}{1-\frac{\gamma_m}{2}G(k_f)\left[\left(\frac{k_x}{k_B}\right)^4+\left(\frac{k_y}{k_B}\right)^4-2\right]}\right\} \qquad \text{(III-1)}$$

$$G(k_f) = \left(\frac{k_fL}{2}\right)\left[\cot\frac{k_fL}{2}+\coth\frac{k_fL}{2}\right] \qquad \text{(III-2)}$$

The limits of the propagation bands corresponding to this wavenumber region can be determined from the poles of Eq. III-1. Thus, examining the denominator we see that for a given value of k_y, we can determine the zeroes in terms of k_x, or setting

$$k_y^4 = 2Bk_B^4 \quad , \quad B \geq 0 \tag{III-3}$$

then we have

$$k_x = \pm \left[2k_B^4\right]^{1/4} \left[\frac{1}{\gamma_m G(k_f)} + 1-B\right]^{1/4} \tag{III-4}$$

now, if the quantity within the brackets of Eq. III-4 is positive then k_x will be wholly real, implying a freely propagating wave. (Alternatively if the term within brackets is negative then clearly,

$$k_x = \pm \frac{k_B}{2^{1/4}} (1+i) \left[\left|\frac{1}{\gamma_m G(k_f)} + 1-B\right|\right]^{1/4} \tag{III-5}$$

and the wave will be damped.

For small values of $\gamma_m(1-B)$ the passband limits are closely approximated by the zeroes of $[G(k_f)]^{-1}$, or

propagating bands, $n\pi \leq \frac{k_f L}{2} \leq \left(\frac{4n+3}{4}\right)\pi$, $n = 0,1,2,3,\ldots,\infty$

nonpropagating bands, $\left(\frac{4n+3}{4}\right)\pi < \frac{k_f L}{2} < (n+1)\pi$, $n = 0,1,2,3,\ldots,\infty$

For other values of $\gamma_m(B-1)$ the plate wavenumber limits of the passbands are best described graphically. This result is depicted in Figure III-1 for several representative values of the beam to plate mass ratio parameter, γ_m. Thus, the left hand graph is a plot of $\gamma_m(B-1)$ vs. B for values of γ_m = 1,5, and 10. The right hand graph is a plot of $[G(k_f)]^{-1}$ vs. $k_f L/2$. As an illustrative example let us assume that we have a structure with $\gamma_m = 1$. Examining Fig. III-1 we see that for k_y wavenumbers much less than the flexural beam wavenumber k_B, the quantity $\gamma_m(B-1)$ is negative and approximately equal to -1, thus real (propagating) values of k_x will result at all frequencies except those at which

$$[G(k_f)]^{-1} < -1$$

Using the right hand chart then we see that this result corresponds to a series of narrow non-propagating bands, each with a lower bound of

$$\frac{k_f L}{2} = \left(\frac{4n+3}{4}\right)\pi$$

For large values of $\frac{k_f L}{2}$ and values of

$$[\gamma_m(B-1)] \leq -1$$

we can determine an approximate value of the bandwidth, Δ_k, from the expression

$$\cot\left[\Delta_k^{NP} + \left(\frac{4n+3}{4}\right)\pi\right] = \left[\frac{k_f L}{2}\ \gamma_m(B-1)\right]^{-1} - 1$$

or

$$\Delta_k^{NP} = \frac{1}{1-k_f L\gamma_m(B-1)}$$

As k_y values nearer to k_B are chosen we see that the bandwidth of the non-propagating bands increases until for,

$$\gamma_m(B-1) > 1$$

most of the frequencies correspond to non-propagating bands with narrow bands of propagating k_x values, each with an upper limit of

$$\frac{k_f L}{2} = \left(\frac{4n+3}{4}\right)\pi$$

The bandwidth in these cases is given by

$$\Delta_k^{P} = \frac{1}{1 + k_f L\gamma_m(B-1)}$$

The essential result of this analysis is that for any given frequency there always exists some set of (k_x,k_y) wavenumbers which freely propagate. This result has been determined from an analysis of the limiting result for $k_f >> k_x,k_y$. Examining the other limiting results, as shown in Fig. II-2, we see that none of the expressions shown indicate passband characteristics.

With a one-dimensional structure, however, the results are somewhat different in that a well defined set of pass-bands does exist. The comparable result from our analysis is that provided by the solution for the point driven one-dimensional array as given by Eq. II-44,

$$\tilde{w}_p(k_x,k_y) = \frac{-F_o}{m_p\omega^2}\left\{\frac{1}{1 - \frac{\gamma_m}{2}\left[\frac{k_fL}{2}\right]\left[\left(\frac{k_y}{k_B}\right)^4 - 1\right]\left[\cot\frac{k_fL}{2} + \coth\frac{k_fL}{2}\right]}\right\}$$

As the grid problem, the limits of the propagation bands are provided by the poles of this expression, or when

$$k_y = k_B\left(\frac{2}{\gamma_m}\right)^{1/4}\left[\frac{1}{G(k_f)} + \frac{\gamma_m}{2}\right]^{1/4} \qquad \text{(III-6)}$$

When the quantity in brackets is negative we will have non-propagating wavenumbers given by

$$k_y = k_B\gamma_m^{-1/4}(1+i)\left[\left|\frac{1}{G(k_f)} + \frac{\gamma_m}{2}\right|\right]^{1/4} \qquad \text{(III-7)}$$

The frequencies at which these will occur are provided by the expression

$$\frac{1}{G(k_f)} \le -\frac{\gamma_m}{2}$$

and from the result for the grid we can write with minor modification.

A. Propagating Bands

1. $\dfrac{\gamma_m}{2} \ll 1$

$$n\pi \leq \frac{k_f L}{2} \leq \left(\frac{4n+3}{4}\right)\pi, \quad n = 0,1,2,\ldots,\infty$$

2. $\dfrac{\gamma_m}{2} \gg 1$

$$0 \leq \frac{k_f L}{2} \leq \frac{3\pi}{4}$$

and

$$\left(\frac{4n+3}{4}\right)\pi + \left(\frac{1}{1 + \frac{k_f L \gamma_m}{2}}\right) \leq \frac{k_f L}{2} \leq \left(\frac{4n+3}{4}\right)\pi, \quad n = 0,1,2,\ldots,\infty$$

B. Non-Propagating Bands

1. $\dfrac{\gamma_m}{2} \ll 1$

$$\left(\frac{4n+3}{4}\right)\pi < \frac{k_f L}{2} < (n+1)\pi, \quad n = 0,1,2,\ldots,\infty$$

2. $\dfrac{\gamma_m}{2} \gg 1$

$$\left(\frac{4n+3}{4}\right)\pi < \frac{k_f L}{2} < \left(\frac{4n+3}{4}\right)\pi + \left[\frac{1}{1 + \frac{k_f L \gamma_m}{2}}\right], \quad n = 0,1,2,\ldots,\infty$$

In comparing this result with the previously cited work by Mead for a one-dimensional beam with a periodic array of rotational restraints, it is noted that the pass-bands just stated for the plate beam array structure

compare with his result for a low rotational inertia--thus, an approximation of a simply supported boundary condition.[5] In this case he shows that the propagation bands are bounded by the n^{th} simply supported resonance on the low side and the n^{th} clamped-clamped resonance on the upper side. Clearly this is very close to the result just obtained in this analysis for the case $\gamma_m = 0$.

A further comparison with Mead results from a comparison with the solution for spring-like as opposed to mass-like constraints. In the former case the pass-bands flip with the result that the clamped-clamped resonances now determine the lower boundary of the pass-bands. An analogous behavior with the grid supported plate is seen when comparing the pass bands in either low or high (k_y/k_B) regions. Thus at low (k_y/k_B) values the structure represents an inertial-like impedance to waves propagating in the x-direction, and at high $k_y/k_B)$ values a compliance like impedance. This analogy becomes somewhat more distinct if we examine the behavior of the $\gamma_m(B-1)$ term in Fig. III-1. Thus, as k_y values from a small fraction of k_B to a large multiple of k_B are traversed we see a clear shift in the sign of the drive point impedance comparable in a qualitative sense to a switch from an inertial to a compliant reactance. It is this periodic shift which directly results in the variance between the one dimensional and two dimensional pass-band results. The relevance of the above results to structure borne noise problems is as follows. For the one dimensional case, the existence of finite band width pass bands and stop bands implies that such a structure can be used as a natural filter to attenuate structure borne noise propagation from a localized excitation. In other words, the one dimensional structure may, in theory, be tuned so that particularly offensive portions of the frequency spectrum of the excitation correspond to stop bands of the structure. However, the two dimensional, or grid, situation is different. Here, there are no stop bands if one assumes that the vibration source exhibits a broad wave-number spectrum such as is produced by a localized vibration source. In other words there is always some portion of the wavenumber spectrum of the excitation that corresponds to a pass-band and thus short circuits the stop band phenomenon. Therefore, in this case, in addition to tuning the frequency

response of the structure to the frequency spectrum of the excitation one must also tune the wavenumber response of the structure to the wavenumber spectrum of the source. Since the wavenumber spectrum of a source is determined largely by the geometrical configuration of its foundation including the structural details of the footings, any attempt to tune a grid structure to take advantage of the existence of stop bands would have to consider such design details.

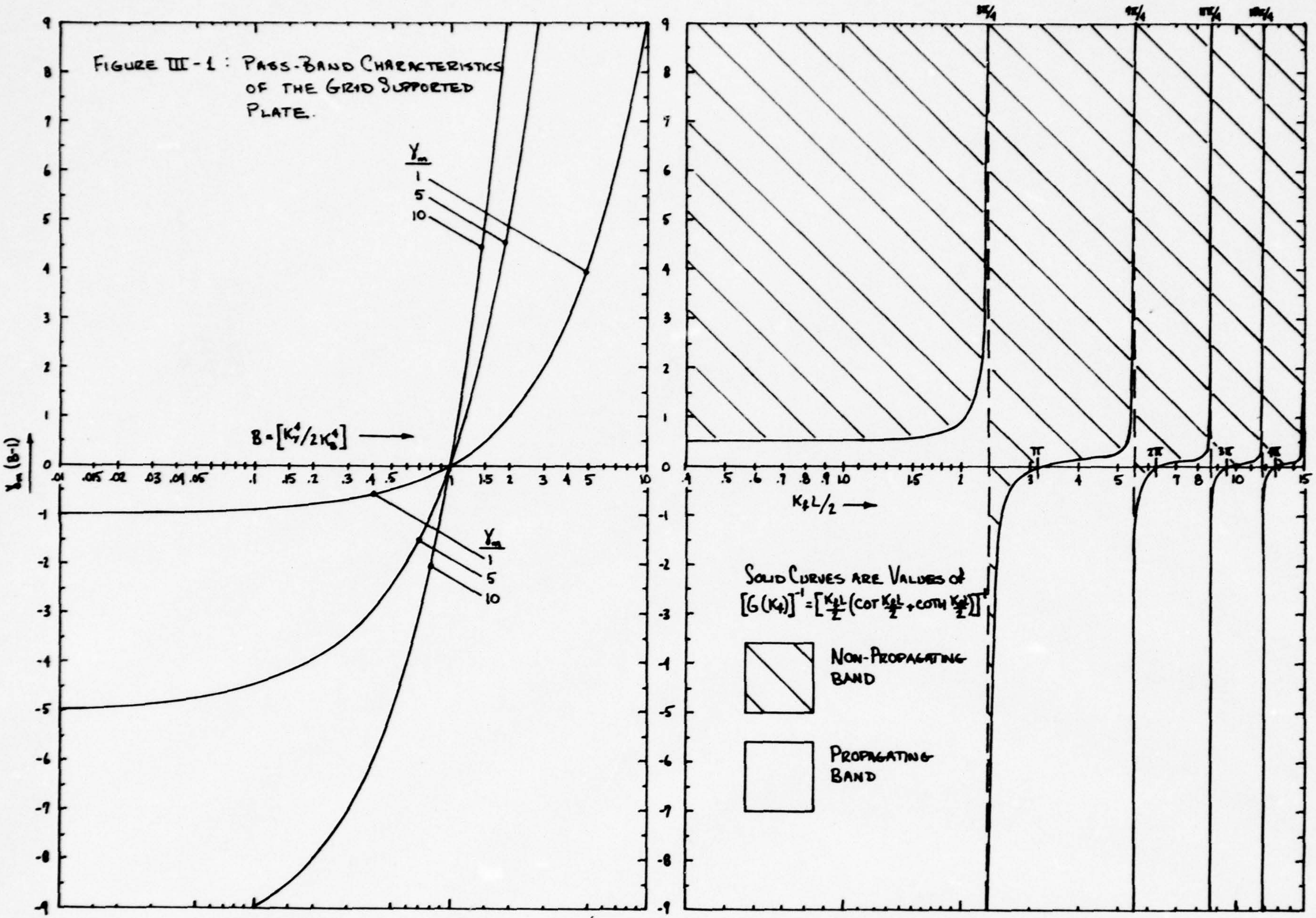

FIGURE III-1: PASS-BAND CHARACTERISTICS OF THE GRID SUPPORTED PLATE.

IV. RADIATED PRESSURE

An interesting and important result directly obtained from the analysis of Section II is the radiated sound pressure measured at a point, (R,θ,ϕ), θ being measured from the normal to the grid or array supported plate and passing through the drive point location. This result can be written as,[6]

$$p(R,\theta,\phi) = -\rho\omega^2 \frac{e^{ikR}}{2\pi R} \tilde{w}(k\sin\theta\cos\phi, k\sin\theta\sin\phi) \tag{IV-1}$$

Thus, if fluid loading is neglected the far field radiated pressure can be developed in a closed-form using Eqs. II-27 and II-32. In the balance of this section we will examine the effect of various structural configurations on the "on-axis" radiated pressure,

$$p(R,0,0) = -\rho\omega^2 \frac{e^{ikR}}{2\pi R} \tilde{w}(0,0)$$

where $\tilde{w}(0,0)$ is given in Eq. II-36. We will compare the resultant radiated pressure from four different structural configurations. In making these comparisons we have used a reference pressure, p_o, equivalent to the high frequency limit for the point driven infinite plate.

$$p_o = \frac{\rho F_o}{m_p} \frac{e^{ikR}}{R} \tag{IV-2}$$

A. Point Driven Infinite Plate

This well known result is given by,

$$\left|\frac{p_\infty(R,0,0)}{p_o}\right| = \frac{\omega m_p}{\rho c}\left[\frac{1}{1+\left(\frac{\omega m_p}{\rho c}\right)^2}\right]^{1/2} \tag{IV-3}$$

$$= \frac{\omega m_p}{\rho c}\ , \quad \omega \to 0 \tag{IV-4}$$

$$= 1\ , \quad \omega \to \infty$$

B. Point Driven Array Supported Plate

Two results are available here, one for the drivepoint at a midspan location,[7] and the one provided by Eq. II-45 for a drivepoint at a beam support location.

1. Mid Span Drive Point

$$\left|\frac{p_{AM}(R,0,0)}{p_o}\right| = \left|\frac{p_\infty(R,0,0)}{p_o}\right| \left\{ 1 - \frac{\dfrac{1}{\sin k_f L/2} + \dfrac{1}{\sinh k_f L/2}}{\dfrac{2}{\gamma_m \dfrac{k_f L}{2}} + \cot\dfrac{k_f L}{2} + \coth\dfrac{k_f L}{2}} \right\} \quad \text{(IV-6)}$$

$$= \frac{\omega m_p}{\rho c}\left[\frac{1}{\gamma_m}\right], \quad \omega \to 0 \quad \text{(IV-7)}$$

$$= 1 - \frac{1}{\cos\left(\dfrac{k_f L}{2}\right) + \sin\left(\dfrac{k_f L}{2}\right)}, \quad \omega \to \infty \quad \text{(IV-8)}$$

2. Beam Drive Point

From Eq. II-45 we can write directly,

$$\left|\frac{p_{AB}(R,0,0)}{p_o}\right| = \left|\frac{p_\infty(R,0,0)}{p_o}\right| \left[\frac{1}{1 + \dfrac{\gamma_m}{2}\dfrac{k_f L}{2}\left(\cot\dfrac{k_f L}{2} + \coth\dfrac{k_f L}{2}\right)}\right] \quad \text{(IV-9)}$$

$$= \frac{\omega m_p}{\rho c}\left[\frac{1}{1+\gamma_m}\right], \quad \omega \to 0 \quad \text{(IV-10)}$$

$$= \frac{\gamma_m}{2}\frac{k_f L}{2}\left[\cot\frac{k_f L}{2} + 1\right], \quad \omega \to \infty \quad \text{(IV-12)}$$

C. Point Driven Grid Supported Plate

As stated in the analysis section the radiated pressure is developed from Eq. II-36. It should benoted that in contrast to the results presented in the analysis section, where the limiting solutions were developed with fluid loading neglected, we have here retained fluid loading to the extent that it is represented in the low frequency limit of the solution. Thus, from Eq. II-8,

$$\left|y_p(0,0)\right| = \frac{1}{L\omega^2 m_p} \frac{p_\infty(R,0,0)}{p_o} \tag{IV-13}$$

Using the transform structural displacement from Eq. II-36 we have for the radiated pressure.

$$\left|\frac{p_G(R,0,0)}{p_o}\right| = \left|\frac{p_\infty(R,0,0)}{p_o}\right| \left\{\frac{1}{1 + \gamma_m \frac{k_f L}{2}\left[\cot\frac{k_f L}{2} \coth\frac{k_f L}{2}\right]}\right\} \tag{IV-14}$$

$$= \frac{\omega m_p}{\rho_c}\left[\frac{1}{1+2\gamma_m}\right] \quad , \ \omega \to 0 \tag{IV-15}$$

$$= \frac{1}{\gamma_m \frac{k_f L}{2}\left(\cot\frac{k_f L}{2} + 1\right)} \quad , \ \omega \to \infty \tag{IV-16}$$

Summaries of these results are shown in Figs. IV-1 and IV-2. The dimensions are typical of airframe structures. A structural damping factor of $\eta_p = .1$ was also used. Several points are of interest to this analysis. At low frequencies the point driven structures differ from the infinite plate result by a factor determined solely by the ratio of beam to plate inertia, γ_m. The actual amounts are shown in each figure.

At high frequencies the point driven structures fall off as 20 log (f) for the beam drive point cases, and approach the infinite plate result, which is frequency independent, for the midspan drive point case. This is due to

the fact that the drive point impedance of a point driven infinite beam is proportional to frequency while that of the infinite plates is frequency independent.

A further point of interest is provided by a comparison with the pass band characteristics determined in Section III. The peaks and valleys in Figs. IV-1 and IV-2 are related to the interframe plating resonances and antiresonances respectively. These plating resonances imply large reactions at the supports adjacent to the drive point which serve to reflect, rather than transmit, incoming waves. Thus the bands corresponding to efficient levels of radiation are very close to the non-propagating bands of the structural analysis.

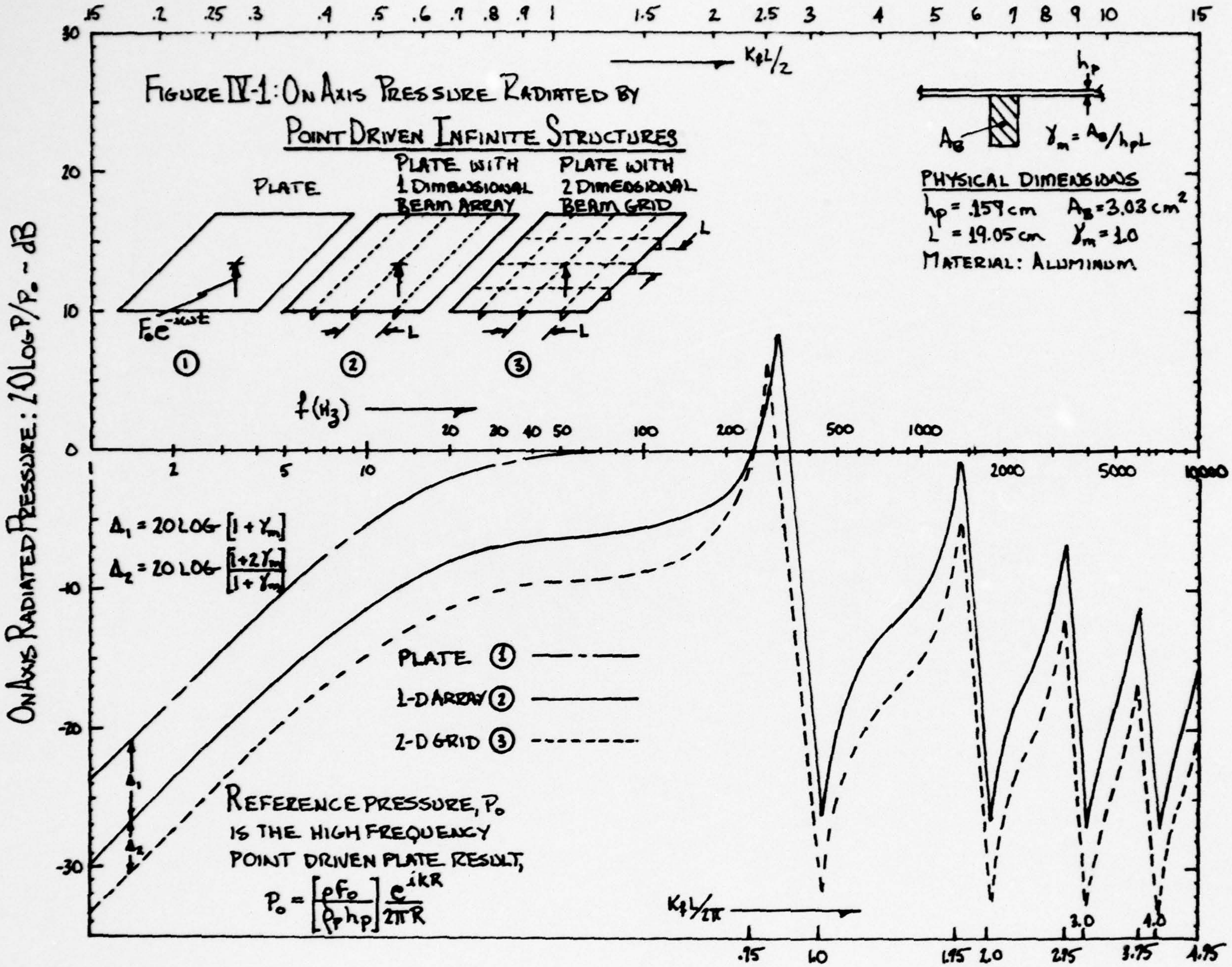

FIGURE IV-1: ON AXIS PRESSURE RADIATED BY POINT DRIVEN INFINITE STRUCTURES

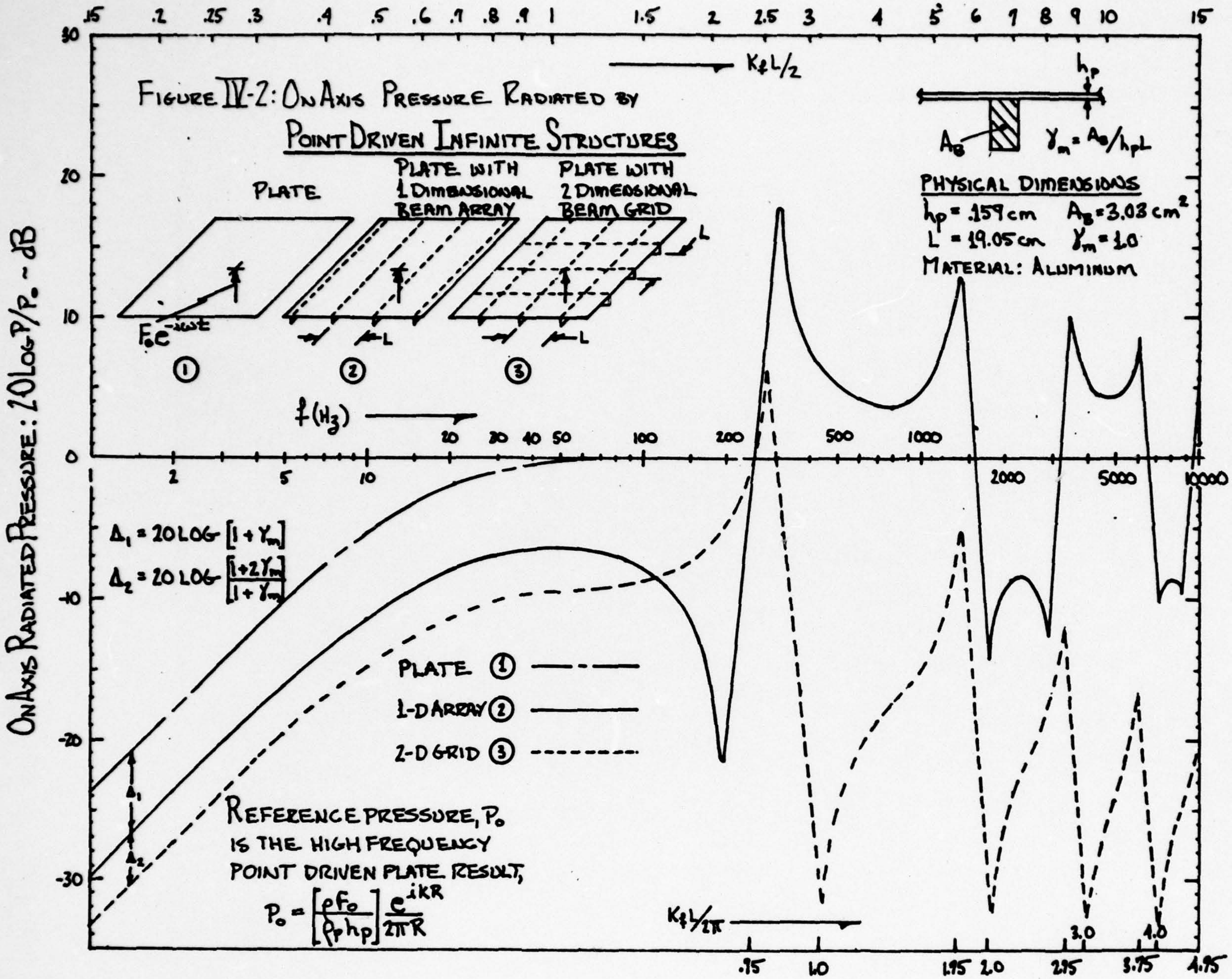

FIGURE IV-2: ON AXIS PRESSURE RADIATED BY POINT DRIVEN INFINITE STRUCTURES

REFERENCES

1 L. Cremer and M. Heckl, Structure-Borne Sound, (Berlin: Springer-Verlag, 1973).

2 D. J. Mead, "Free Wave Propagation in Periodically Supported, Infinite Beams," J. Sound and Vibration 11, 181-191 (1970).

3 M. C. Junger and D. L. Feit, Sound, Structures and Their Interaction, (M.I.T. Press, Cambridge, 1972) p. 96, Eq. 5.35, 5.35a.

4 M. R. Spiegel, Theory and Problems of Complex Variables, (McGraw-Hill, New York, 1964), Chapt. 7.

5 D. J. Mead, Op Cit.

6 M. C. Junger and D. L. Feit, Op. Cit., p. 94, Eq. 5.31.

7 J. M. Garrelick and G.-F. Lin, "Effect of the Number of Frames on the Sound Radiated by Fluid-Loaded, Frame-Stiffened Plates," J. Acoust. Soc. Am. 58, 2, (Aug. 1975), p. 499.

474:NP:716:lab
78u474-619

ONR Code 474
August 1979

DISTRIBUTION LIST

for

UNCLASSIFIED TECHNICAL REPORTS

The ONR Structural Mechanics Contract Research Program

This list consists of:

Part 1 - Government Activities
Part 2 - Contractors and Other
Technical Collaborators

Notes:

Except as otherwise indicated, forward one copy of all Unclassified Technical Reports to each of the addressees listed herein.

Where more than one attention addressee is indicated, the individual copies of the report should be mailed separately.

Part 1 - Government
Administrative and Liaison Activities

Office of Naval Research
Department of the Navy
Arlington, Virginia 22217
Attn: Code 474 (2)
Code 471
Code 200

Director
Office of Naval Research
Branch Office
666 Summer Street
Boston, Massachusetts 02210

Director
Office of Naval Research
Branch Office
536 South Clark Street
Chicago, Illinois 60605

Director
Office of Naval Research
New York Area Office
715 Broadway - 5th Floor
New York, New York 10003

Director
Office of Naval Research
Branch Office
1030 East Green Street
Pasadena, California 91106

Naval Research Laboratory (6)
Code 2627
Washington, D.C. 20375

Defense Documentation Center (12)
Cameron Station
Alexandria, Virginia 22314

Navy

Undersea Explosion Research Division
Naval Ship Research and Development Center
Norfolk Naval Shipyard
Portsmouth, Virginia 23709
Attn: Dr. E. Palmer, Code 177

Navy (Con't.)

Naval Research Laboratory
Washington, D.C. 20375
Attn: Code 8400
8410
8430
8440
6300
6390
6380

David W. Taylor Naval Ship Research and Development Center
Annapolis, Maryland 21402
Attn: Code 2740
28
281

Naval Weapons Center
China Lake, California 93555
Attn: Code 4062
4520

Commanding Officer
Naval Civil Engineering Laboratory
Code L31
Port Hueneme, California 93041

Naval Surface Weapons Center
White Oak
Silver Spring, Maryland 20910
Attn: Code R-10
G-402
K-82

Technical Director
Naval Ocean Systems Center
San Diego, California 92152

Supervisor of Shipbuilding
U.S. Navy
Newport News, Virginia 23607

Navy Underwater Sound Reference Division
Naval Research Laboratory
P.O. Box 8337
Orlando, Florida 32806

Navy (Con't.)

Chief of Naval Operations
Department of the Navy
Washington, D.C. 20350
Attn: Code OP-098

Strategic Systems Project Office
Department of the Navy
Washington, D.C. 20376
Attn: NSP-200

Naval Air Systems Command
Department of the Navy
Washington, D.C. 20361
Attn: Code 5302 (Aerospace and Structures)
604 (Technical Library)
320B (Structures)

Naval Air Development Center
Warminster, Pennsylvania 18974
Attn: Aerospace Mechanics
Code 606

U.S. Naval Academy
Engineering Department
Annapolis, Maryland 21402

Naval Facilities Engineering Command
200 Stovall Street
Alexandria, Virginia 22332
Attn: Code 03 (Research and Development)
04B
045
14114 (Technical Library)

Naval Sea Systems Command
Department of the Navy
Washington, D.C. 20362
Attn: Code 05H
312
322
323
05R
32R

Navy (Con't.)

Commander and Director
David W. Taylor Naval Ship
Research and Development Center
Bethesda, Maryland 20084
Attn: Code 042
17
172
173
174
1800
1844
012.2
1900
1901
1945
1960
1962

Naval Underwater Systems Center
Newport, Rhode Island 02840
Attn: Dr. R. Trainor

Naval Surface Weapons Center
Dahlgren Laboratory
Dahlgren, Virginia 22448
Attn: Code G04
G20

Technical Director
Mare Island Naval Shipyard
Vallejo, California 94592

U.S. Naval Postgraduate School
Library
Code 0384
Monterey, California 93940

Webb Institute of Naval Architecture
Attn: Librarian
Crescent Beach Road, Glen Cove
Long Island, New York 11542

Army

Commanding Officer (2)
U.S. Army Research Office
P.O. Box 12211
Research Triangle Park, NC 27709
Attn: Mr. J. J. Murray, CRD-AA-IP

Army (Con't.)

Watervliet Arsenal
MAGGS Research Center
Watervliet, New York 12189
Attn: Director of Research

U.S. Army Materials and Mechanics
Research Center
Watertown, Massachusetts 02172
Attn: Dr. R. Shea, DRXMR-T

U.S. Army Missile Research and
Development Center
Redstone Scientific Information
Center
Chief, Document Section
Redstone Arsenal, Alabama 35809

Army Research and Development
Center
Fort Belvoir, Virginia 22060

NASA

National Aeronautics and Space
Administration
Structures Research Division
Langley Research Center
Langley Station
Hampton, Virginia 23365

National Aeronautics and Space
Administration
Associate Administrator for Advanced
Research and Technology
Washington, D.C. 20546

Air Force

Wright-Patterson Air Force Base
Dayton, Ohio 45433
Attn: AFFDL (FB)
(FBR)
(FBE)
(FBS)
AFML (MBM)

Air Force (Con't.)

Chief Applied Mechanics Group
U.S. Air Force Institute of Technology
Wright-Patterson Air Force Base
Dayton, Ohio 45433

Chief, Civil Engineering Branch
WLRC, Research Division
Air Force Weapons Laboratory
Kirtland Air Force Base
Albuquerque, New Mexico 87117

Air Force Office of Scientific Research
Bolling Air Force Base
Washington, D.C. 20332
Attn: Mechanics Division

Department of the Air Force
Air University Library
Maxwell Air Force Base
Montgomery, Alabama 36112

Other Government Activities

Commandant
Chief, Testing and Development Division
U.S. Coast Guard
1300 E Street, NW.
Washington, D.C. 20226

Technical Director
Marine Corps Development
and Education Command
Quantico, Virginia 22134

Director Defense Research
and Engineering
Technical Library
Room 3C128
The Pentagon
Washington, D.C. 20301

Other Government Activities (Con't)

Dr. M. Gaus
National Science Foundation
Environmental Research Division
Washington, D.C. 20550

Library of Congress
Science and Technology Division
Washington, D.C. 20540

Director
Defense Nuclear Agency
Washington, D.C. 20305
Attn: SPSS

Mr. Jerome Persh
Staff Specialist for Materials
and Structures
OUSDR&E, The Pentagon
Room 3D1089
Washington, D.C. 20301

Chief, Airframe and Equipment Branch
FS-120
Office of Flight Standards
Federal Aviation Agency
Washington, D.C. 20553

National Academy of Sciences
National Research Council
Ship Hull Research Committee
2101 Constitution Avenue
Washington, D.C. 20418
Attn: Mr. A. R. Lytle

National Science Foundation
Engineering Mechanics Section
Division of Engineering
Washington, D.C. 20550

Picatinny Arsenal
Plastics Technical Evaluation Center
Attn: Technical Information Section
Dover, New Jersey 07801

Maritime Administration
Office of Maritime Technology
14th and Constitution Avenue, NW.
Washington, D.C. 20230

PART 2 - Contractors and Other Technical Collaborators

Universities

Dr. J. Tinsley Oden
University of Texas at Austin
345 Engineering Science Building
Austin, Texas 78712

Professor Julius Miklowitz
California Institute of Technology
Division of Engineering
and Applied Sciences
Pasadena, California 91109

Dr. Harold Liebowitz, Dean
School of Engineering and
Applied Science
George Washington University
Washington, D.C. 20052

Professor Eli Sternberg
California Institute of Technology
Division of Engineering and
Applied Sciences
Pasadena, California 91109

Professor Paul M. Naghdi
University of California
Department of Mechanical Engineering
Berkeley, California 94720

Professor A. J. Durelli
Oakland University
School of Engineering
Rochester, Missouri 48063

Professor F. L. DiMaggio
Columbia University
Department of Civil Engineering
New York, New York 10027

Professor Norman Jones
The University of Liverpool
Department of Mechanical Engineering
P. O. Box 147
Brownlow Hill
Liverpool L69 3BX
England

Professor E. J. Skudrzyk
Pennsylvania State University
Applied Research Laboratory
Department of Physics
State College, Pennsylvania 16801

Universities (Con't.)

Professor J. Klosner
Polytechnic Institute of New York
Department of Mechanical and
Aerospace Engineering
333 Jay Street
Brooklyn, New York 11201

Professor R. A. Schapery
Texas A&M University
Department of Civil Engineering
College Station, Texas 77843

Professor Walter D. Pilkey
University of Virginia
Research Laboratories for the
Engineering Sciences and
Applied Sciences
Charlottesville, Virginia 22901

Professor K. D. Willmert
Clarkson College of Technology
Department of Mechanical Engineering
Potsdam, New York 13676

Dr. Walter E. Haisler
Texas A&M University
Aerospace Engineering Department
College Station, Texas 77843

Dr. Hussein A. Kamel
University of Arizona
Department of Aerospace and
Mechanical Engineering
Tucson, Arizona 85721

Dr. S. J. Fenves
Carnegie-Mellon University
Department of Civil Engineering
Schenley Park
Pittsburgh, Pennsylvania 15213

Dr. Ronald L. Huston
Department of Engineering Analysis
University of Cincinnati
Cincinnati, Ohio 45221

Universities (Con't)

Professor G. C. M. Sih
Lehigh University
Institute of Fracture and
Solid Mechanics
Bethlehem, Pennsylvania 18015

Professor Albert S. Kobayashi
University of Washington
Department of Mechanical Engineering
Seattle, Washington 98105

Professor Daniel Frederick
Virginia Polytechnic Institute and
State University
Department of Engineering Mechanics
Blacksburg, Virginia 24061

Professor A. C. Eringen
Princeton University
Department of Aerospace and
Mechanical Sciences
Princeton, New Jersey 08540

Professor E. H. Lee
Stanford University
Division of Engineering Mechanics
Stanford, California 94305

Professor Albert I. King
Wayne State University
Biomechanics Research Center
Detroit, Michigan 48202

Dr. V. R. Hodgson
Wayne State University
School of Medicine
Detroit, Michigan 48202

Dean B. A. Boley
Northwestern University
Department of Civil Engineering
Evanston, Illinois 60201

Universities (Con't)

Professor P. G. Hodge, Jr.
University of Minnesota
Department of Aerospace Engineering
and Mechanics
Minneapolis, Minnesota 55455

Dr. D. C. Drucker
University of Illinois
Dean of Engineering
Urbana, Illinois 61801

Professor N. M. Newmark
University of Illinois
Department of Civil Engineering
Urbana, Illinois 61803

Professor E. Reissner
University of California, San Diego
Department of Applied Mechanics
La Jolla, California 92037

Professor William A. Nash
University of Massachusetts
Department of Mechanics and
Aerospace Engineering
Amherst, Massachusetts 01002

Professor G. Herrmann
Stanford University
Department of Applied Mechanics
Stanford, California 94305

Professor J. D. Achenbach
Northwest University
Department of Civil Engineering
Evanston, Illinois 60201

Professor S. B. Dong
University of California
Department of Mechanics
Los Angeles, California 90024

Professor Burt Paul
University of Pennsylvania
Towne School of Civil and
Mechanical Engineering
Philadelphia, Pennsylvania 19104

Universities (Con't)

Professor H. W. Liu
Syracuse University
Department of Chemical Engineering
and Metallurgy
Syracuse, New York 13210

Professor S. Bodner
Technion R&D Foundation
Haifa, Israel

Professor Werner Goldsmith
University of California
Department of Mechanical Engineering
Berkeley, California 94720

Professor R. S. Rivlin
Lehigh University
Center for the Application
of Mathematics
Bethlehem, Pennsylvania 18015

Professor F. A. Cozzarelli
State University of New York at
Buffalo
Division of Interdisciplinary Studies
Karr Parker Engineering Building
Chemistry Road
Buffalo, New York 14214

Professor Joseph L. Rose
Drexel University
Department of Mechanical Engineering
and Mechanics
Philadelphia, Pennsylvania 19104

Professor B. K. Donaldson
University of Maryland
Aerospace Engineering Department
College Park, Maryland 20742

Professor Joseph A. Clark
Catholic University of America
Department of Mechanical Engineering
Washington, D.C. 20064

Universities (Con't)

Dr. Samuel B. Batdorf
University of California
School of Engineering
and Applied Science
Los Angeles, California 90024

Professor Isaac Fried
Boston University
Department of Mathematics
Boston, Massachusetts 02215

Professor E. Krempl
Rensselaer Polytechnic Institute
Division of Engineering
Engineering Mechanics
Troy, New York 12181

Dr. Jack R. Vinson
University of Delaware
Department of Mechanical and Aerospace
Engineering and the Center for
Composite Materials
Newark, Delaware 19711

Dr. J. Duffy
Brown University
Division of Engineering
Providence, Rhode Island 02912

Dr. J. L. Swedlow
Carnegie-Mellon University
Department of Mechanical Engineering
Pittsburgh, Pennsylvania 15213

Dr. V. K. Varadan
Ohio State University Research Foundation
Department of Engineering Mechanics
Columbus, Ohio 43210

Dr. Z. Hashin
University of Pennsylvania
Department of Metallurgy and
Materials Science
College of Engineering and
Applied Science
Philadelphia, Pennsylvania 19104

Universities (Con't)

Dr. Jackson C. S. Yang
University of Maryland
Department of Mechanical Engineering
College Park, Maryland 20742

Professor T. Y. Chang
University of Akron
Department of Civil Engineering
Akron, Ohio 44325

Professor Charles W. Bert
University of Oklahoma
School of Aerospace, Mechanical,
and Nuclear Engineering
Norman, Oklahoma 73019

Professor Satya N. Atluri
Georgia Institute of Technology
School of Engineering and
Mechanics
Atlanta, Georgia 30332

Professor Graham F. Carey
University of Texas at Austin
Department of Aerospace Engineering
and Engineering Mechanics
Austin, Texas 78712

Dr. S. S. Wang
University of Illinois
Department of Theoretical and
Applied Mechanics
Urbana, Illinois 61801

Industry and Research Institutes

Dr. Norman Hobbs
Kaman AviDyne
Division of Kaman
Sciences Corporation
Burlington, Massachusetts 01803

Argonne National Laboratory
Library Services Department
9700 South Cass Avenue
Argonne, Illinois 60440

Industry and Research Institutes (Con't)

Dr. M. C. Junger
Cambridge Acoustical Associates
54 Rindge Avenue Extension
Cambridge, Massachusetts 02140

Dr. V. Godino
General Dynamics Corporation
Electric Boat Division
Groton, Connecticut 06340

Dr. J. E. Greenspon
J. G. Engineering Research Associates
3831 Menlo Drive
Baltimore, Maryland 21215

Newport News Shipbuilding and
Dry Dock Company
Library
Newport News, Virginia 23607

Dr. W. F. Bozich
McDonnell Douglas Corporation
5301 Bolsa Avenue
Huntington Beach, California 92647

Dr. H. N. Abramson
Southwest Research Institute
8500 Culebra Road
San Antonio, Texas 78284

Dr. R. C. DeHart
Southwest Research Institute
8500 Culebra Road
San Antonio, Texas 78284

Dr. M. L. Baron
Weidlinger Associates
110 East 59th Street
New York, New York 10022

Dr. T. L. Geers
Lockheed Missiles and Space Company
3251 Hanover Street
Palo Alto, California 94304

Mr. William Caywood
Applied Physics Laboratory
Johns Hopkins Road
Laurel, Maryland 20810

Industry and Research Institutes (Con't)

Dr. Robert E. Dunham
Pacifica Technology
P.O. Box 148
Del Mar, California 92014

Dr. M. F. Kanninen
Battelle Columbus Laboratories
505 King Avenue
Columbus, Ohio 43201

Dr. A. A. Hochrein
Daedalean Associates, Inc.
Springlake Research Road
15110 Frederick Road
Woodbine, Maryland 21797

Dr. James W. Jones
Swanson Service Corporation
P.O. Box 5415
Huntington Beach, California 92646

Dr. Robert E. Nickell
Applied Science and Technology
3344 North Torrey Pines Court
Suite 220
La Jolla, California 92037

Dr. Kevin Thomas
Westinghouse Electric Corp.
Advanced Reactors Division
P. O. Box 158
Madison, Pennsylvania 15663